



LAWRENCE
LIVERMORE
NATIONAL
LABORATORY

LLNL-TR-406844

Probing other solar systems with current and future adaptive optics

B. Macintosh, C. Marois, D. Phillion, L. Poyneer, J. Graham, B. Zuckerman, D. Gavel, J.-P. Veran, J. Wilhelmsen-Evans, C. Mellis

September 9, 2008

Disclaimer

This document was prepared as an account of work sponsored by an agency of the United States government. Neither the United States government nor Lawrence Livermore National Security, LLC, nor any of their employees makes any warranty, expressed or implied, or assumes any legal liability or responsibility for the accuracy, completeness, or usefulness of any information, apparatus, product, or process disclosed, or represents that its use would not infringe privately owned rights. Reference herein to any specific commercial product, process, or service by trade name, trademark, manufacturer, or otherwise does not necessarily constitute or imply its endorsement, recommendation, or favoring by the United States government or Lawrence Livermore National Security, LLC. The views and opinions of authors expressed herein do not necessarily state or reflect those of the United States government or Lawrence Livermore National Security, LLC, and shall not be used for advertising or product endorsement purposes.

This work performed under the auspices of the U.S. Department of Energy by Lawrence Livermore National Laboratory under Contract DE-AC52-07NA27344.

FY07 LDRD Final Report
Probing other solar systems with current and
future adaptive optics
05-ERD-055
LLNL-TR-406844
Bruce Macintosh

Principal Investigator: Bruce Macintosh, I Division (PAT Directorate) and
Institute of Geophysics and Planetary Physics

Co-Investigators: Christian Marois, IGPP
Don Phillion, I Division
Lisa Poyneer, I Division

University Collaborators: Prof. James Graham, UC Berkeley
Prof. Ben Zuckerman, UCLA
Donald Gavel, Director, Laboratory for Adaptive Optics,
UCSC
Jean-Pierre Veran, Herzberg Institute of Astrophysics,
Canada

Students: Julia Wilhelmsen-Evans, UC Davis
Carl Mellis, UCLA

ABSTRACT:

Over the past decade, the study of extrasolar planets through indirect techniques – primarily Doppler measurements – has revolutionized our understanding of other solar systems. The next major step in this field will be the direct detection and characterization, via imaging and spectroscopy, of the planets themselves. To achieve this, we must separate the light from the faint planet from the extensive glare of its parent star. We pursued this goal using the current generation of adaptive optics (AO) systems on large ground-based telescopes, using infrared imaging to search for the thermal emission from young planets and developing image processing techniques to distinguish planets from telescope-induced artifacts. Our new Angular Differential Imaging (ADI) technique, which uses the sidereal rotation of the Earth and telescope, is now standard for ground-based high-contrast imaging. Although no young planets were found in our surveys, we placed the strongest limits yet on giant planets in wide orbits (>30 AU) around young stars and characterized planetary companion candidates.

The imaging of planetary companions on solar-system-like scales (5-30 AU) will require a new generation of advanced AO systems that are an order of magnitude more powerful than the LLNL-built Keck AO system. We worked to develop and test the key

technologies needed for these systems, including a spatially-filtered wavefront sensor, efficient and accurate wavefront reconstruction algorithms, and precision AO wavefront control at the sub-nm level. LLNL has now been selected by the Gemini Observatory to lead the construction of the Gemini Planet Imager, a \$24M instrument that will be the most advanced AO system in the world.

1. Introduction and scientific motivation

For the first time in history, indirect detection techniques have permitted astronomers to explore the environments of nearby stars on scales comparable to the size of our solar system. The most powerful approach to date has been the study of the Doppler shift induced by the gravitational effects of planets on their parent star. The planets themselves, however, can only be directly studied in the extremely rare circumstance where their orbit is aligned with the Earth. These techniques, though powerful, are sensitive only to planets that are very close to their parent star, and for the most part measure only the most basic properties of a planet – its mass and orbital separation.

Discoveries of extrasolar planets have galvanized public interest in science and technology and have led to profound new insights into the formation and evolution of planetary systems, and they have set the stage for the next step: direct detection characterization of extrasolar Jovian planets. **Direct** imaging detection of such planets is barely within the reach of current telescopes and adaptive optics (AO) systems, only if the planets are young (and hence bright) and orbiting at the edge of their solar systems. To truly probe the environments of other stars on scales comparable to the size of our solar system will require the development of next-generation dedicated high-contrast adaptive optics systems, sometimes referred to as “Extreme” adaptive optics (ExAO). With its world-class expertise in AO and precision optical systems, LLNL has lead this area within the US astronomical community.

During the course of this project we applied a two-pronged approach to advancing the study of extrasolar planetary systems. First, we used AO on the current generation of large telescopes to probe nearby stars, studying both the circumstellar dust disks that form planets and the planets that may be shaping those disks. In support of this, we developed image analysis tools needed to distinguish planetary systems from the complex noise of scattered light induced by the telescope and atmosphere. Although our direct imaging search to date has detected no extrasolar planets, we have studied several unique systems that may be in the process of producing planets, and the image processing techniques we developed have now become standard in the field.

Second, we developed the technologies needed for the future planet-hunting ExAO systems (Figure 1), particularly the ability to control and calibrate an adaptive optics system with thousands of actuators at nanometer levels of precision. Ultimately, a LLNL-led team was selected by the international Gemini Observatory to build such a system, the Gemini Planet Imager, incorporating the techniques developed by this LDRD.

Adaptive optics is a key technological expertise for many LLNL programmatic applications as well. The advanced adaptive optics concepts developed here will be

applied in the future to a wide range of non-astronomical applications such as remote sensing, biomedical microscopy, and laser beam control.

2. Studying other solar systems with current adaptive optics systems

The direct detection of components of other solar systems is one of the most challenging problems in modern astronomy. To place the problem in perspective, Jupiter, seen by an observer at the nearby star Vega, would be one billion times fainter than the sun and separated by an angle of half a second of arc. We refer to this as the *contrast*: the ratio of brightness between a planet and its parent star. A mature Jupiter-like planet at an orbital separation of 5 astronomical units (AU) has a contrast of 10^{-9} . When we observe a bright star with a conventional telescope, light from the star is scattered by turbulence in the Earth's atmosphere, diffraction from the finite telescope aperture, imperfections in the optics of the telescope, etc., and completely swamps the faint signal of any planets.

To truly overcome this will require the application of a variety of advanced optical techniques in an integrated system design (Section 4.) In the nearer term, however, we can apply careful image processing to existing telescopes and instruments. AO can partially correct for the scattering by the atmosphere. For example, the LLNL-built adaptive optics system on the 10-m W.M. Keck II telescope is the world's most advanced astronomical system on the world's largest optical/IR telescope and produces high resolution images at near-infrared wavelengths. Its correction is still imperfect, and aberrations in the telescope itself will result in artifacts that can hide the planet. We developed an image processing technique (Section 2.1) that takes advantage of the rotation of the Earth and telescope to partially distinguish between planets and artifacts.

Using these techniques we can achieve contrasts of 10^{-5} to 10^{-6} at separations of about one arcsecond. While this is insufficient to detect a solar system exactly like our own, it would allow us to detect young planets. When a giant planet forms from a contraction or accretion of protoplanetary gas, gravitational potential energy is released. Depending on the exact formation history, the planet may retain a significant fraction of this energy and stay warm for a long period. The planet will be more detectable at infrared wavelengths, because the contrast between the radiation emitted by the warm planet and the star is much more favorable. For mature planets, the reflected light contrast is more severe. Because planets are thought to form not long after their stars do, surveys of young stars have the greatest potential to see associated planets. We participated in several such surveys (see Section 2.3.) Unfortunately, young stars are rare, and hence will be more distant from the Earth – reducing the angular separation between a given planet and star as seen from the Earth. As a result, we are sensitive primarily to planets in wide orbits (>20 AU), corresponding to the outer parts of our solar system.

2.1. Angular Differential Imaging

As discussed above, stars (seen through a telescope) are surrounded by a halo of scattered light, referred to as the Point Spread Function (PSF). A major source of such scattered light is optical aberrations (uncorrectable by adaptive optics) on telescope and instrument mirrors. Since starlight is coherent, light scattered by these aberrations

produces a pattern of speckles (as would a laser) that easily swamp the signal from a planet. Atmospheric wavefront errors also produce a speckle pattern, but since atmospheric phase errors vary randomly during the observation, this pattern tends to smooth out over time. Speckles from optical aberrations will remain present on the timescales that the optics are stable for. Typically this is several minutes – long enough to swamp a planetary signal but too short to allow the telescope to acquire separate measurements of a reference star.

One way to overcome this is to use the star itself for self-referencing by taking advantage of the rotation of the earth and telescope. When a modern altitude/azimuth telescope tracks a celestial object, the field of view rotates on the final focal plane. Normally this rotation is compensated for by counter-rotating the science camera. If this counter-rotator is disabled, the camera remains fixed with respect to the telescope. This causes any PSF artifacts from the telescope, camera optics, or combinations thereof to remain fixed and steady while a planetary companion will rotate about the center of the image. Taking a series of short (1 minute) exposures and subtracting suitably spaced images from each other, we can remove artifacts without eliminating the planet signal. The subtracted images can then be derotated and combined in software (Figure 1.)

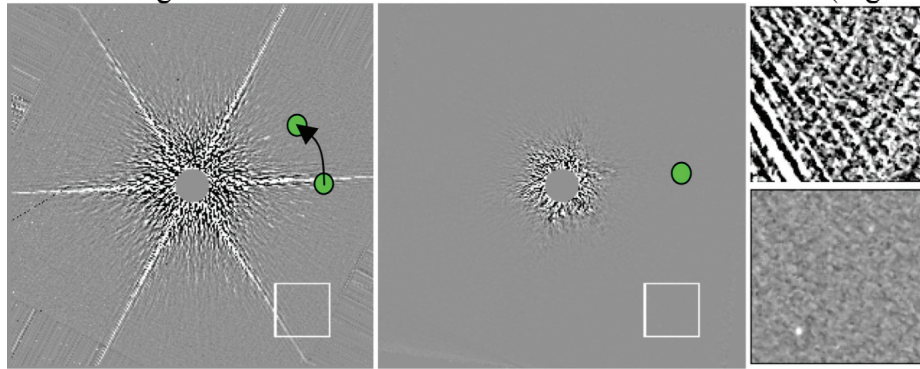


Figure 1: Principal of angular differential imaging (ADI). Left: A single Keck AO image of a bright star. The image has been high-pass filtered to remove the smooth part of the halo, leaving a bright and dark speckle pattern. If the science camera is held fixed with respect to the telescope, a planetary companion will rotate on the field of view as the Earth rotates; speckle artifacts remain fixed. By taking a series of short exposure images and subtracting them, these artifacts can be attenuated (center). The images can then be derotated in software and combined to reveal the planet. Right: close-up of a small region of the single raw image (top) and average of many images after ADI processing (bottom).

This technique, now known as Angular Differential Imaging (ADI) was independently proposed by Bruce Macintosh (LLNL) and Christian Marois (during his Ph.D. thesis work at University of Montreal before his postdoctoral employment at LLNL.) A simpler technique had been applied the Hubble Space Telescope by rotating the spacecraft itself. (Lowrance et al 2005) During the course of this LDRD, Marois developed the formal framework and software pipeline for analyzing ADI data (Marois et al 2006). The enhancement in sensitivity, particularly for companions at wide separations, is 10 to 100 times. Using this technique the Keck AO system substantially exceeds the sensitivity of even the Hubble Space telescope. The technique is now in routine use by all groups carrying out high-contrast imaging (LaFreniere et al 2007;

Fitzgerald et al 2007; Apai et al 2007; and many others) and will be a key tool in future exoplanet surveys (see section 4).

2.2. Reference grids for high-contrast observations

Knowing the position of the bright central star in high-contrast images is crucial both to initial analysis (to allow shifts and rotation of the data as discussed above) and to scientific interpretation of any candidate companions. A key diagnostic to distinguish true companions from background stars is a measurement of its relative position: a true companion will co-move through time with the parent star while a more distant background object will most likely have a much smaller motion. Another key diagnostic is a measurement of its brightness, which is typically done relative to the parent star. Since the parent star usually saturates the imaging detector and/or is hidden behind occulting masks, these measurements are necessarily imprecise – they must be done by interleaving unsaturated/unocculted images with longer high-sensitivity exposures.

We developed a technique to overcome this problem. By inserting a grid into the pupil (e.g. at the deformable mirror), a set of “ghost” images of the primary star are generated (as by a diffraction grating.) The properties of this grid can be tuned to adjust the relative brightness and spacing of the satellite images. The images will then track the position, Strehl ratio and intensity of the saturated/occulted primary star image (Marois et al 2006b)

2.3. Survey results

In collaboration with a team at UCLA, we used the Keck telescope to survey ~100 young (8-100 Myr) nearby (10-100 pc) stars for planetary companions. No true companions were found. A separate collaboration with University of Montreal (Lafreniere et al 2007) surveying a slightly older sample of 85 stars using the Gemini telescope also produced no detections. As discussed above, these surveys are sensitive only to planets only in wide orbits (>40 AU) but now produce strong constraints on the existence of those planets – at the 95% confidence level, no more than 9% of stars have a planet with mass between 0.5 and 13 Jupiter masses in 50-250 AU separations. (For comparison, the semi-major axis of Pluto’s orbit in our solar system is 40 AU.) This in turn constrains models of planet formation; the planet-forming disks around young stars are often observed to be >100 AU in radius, but those disks apparently only succeed in forming giant planets in their inner regions.

We also participated in a University of Arizona / UCLA survey using the Keck AO system’s Laser Guide Star mode to observe brown dwarfs (“failed stars”, objects whose mass is too low to sustain thermonuclear fusion.) Since these objects are intrinsically much fainter than stars, planetary companions would be easier to detect. We discovered that several brown dwarfs previously identified as single objects were in fact lower-mass double systems, though none were of truly planetary mass. (Close et al 2007, Siegler et al 2007.)

To truly constrain planet populations on the scales where the giant planets of our solar system are found (5-30 AU) will require new instruments such as the Gemini Planet Imager (Section 4.)

2.4. Characterization of candidate extrasolar planets

The field of direct imaging has been marked by a series of claims of detected extrasolar planets, most of which ultimately prove to be false; the proposed companion is either a unrelated background object (e.g. Terebey et al 2000) or a higher-mass objects such as a brown dwarf.

One such claim was made for the low-mass companion to the star GQ Lup (Neuhauser et al 2005), imaged with AO by the European Very Large Telescope. The interpretation of this as a planetary-mass companion hinged on attempts to measure its temperature and luminosity using low-SNR spectra and on a particular set of theoretical models. Using our expertise in image processing, we extracted accurate measurements of the object's brightness from archival images spanning the range from 0.5 – 4 microns, allowing us to much more narrowly contain the object's temperature and radius. In the process, we discovered errors in the photometry and luminosity estimates of the original author and securely established that the object is a brown dwarf rather than stellar companion (Marois et al. 2007). Figure 2 and Figure 3 show the results. We also show evidence that this object is still accreting mass and may end up even more massive.

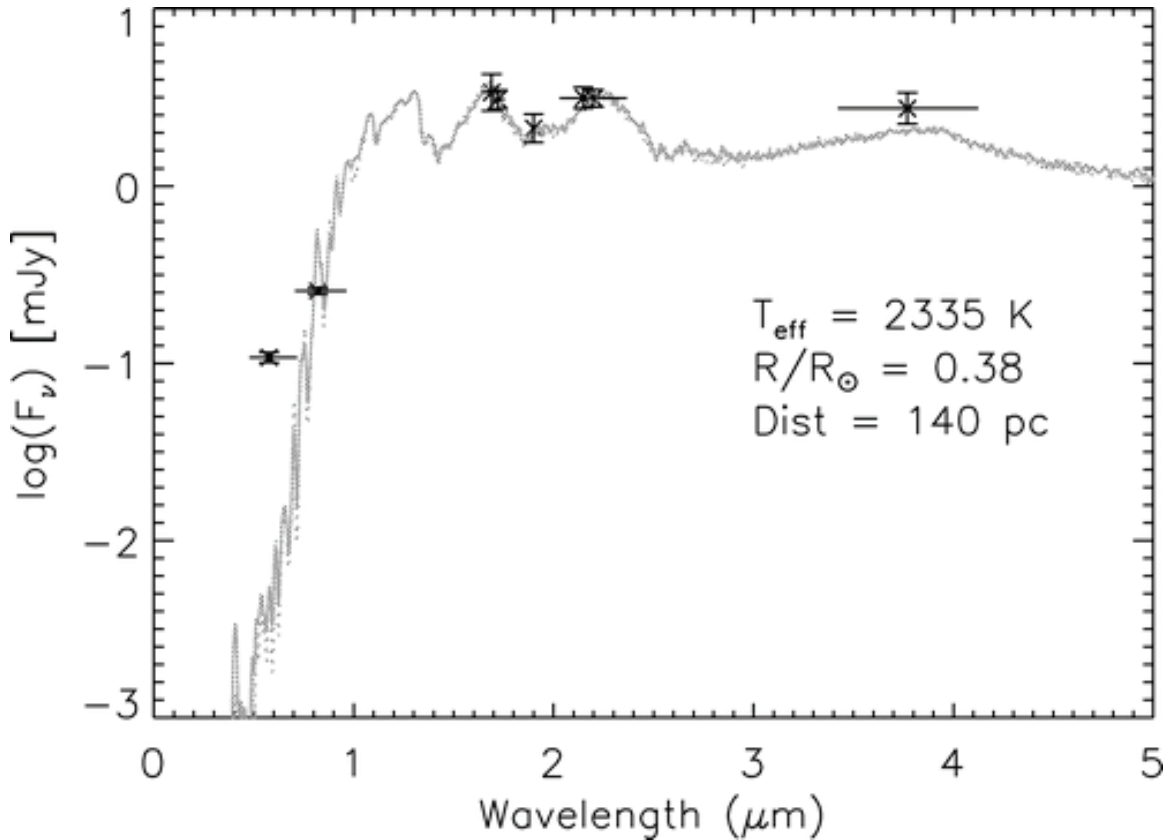


Figure 2: Photometric measurements of the brightness of the candidate planet GQ Lup (symbols) together with best-fit spectrum. The excess at 0.6 microns is likely caused by H-alpha emission from accreting gas

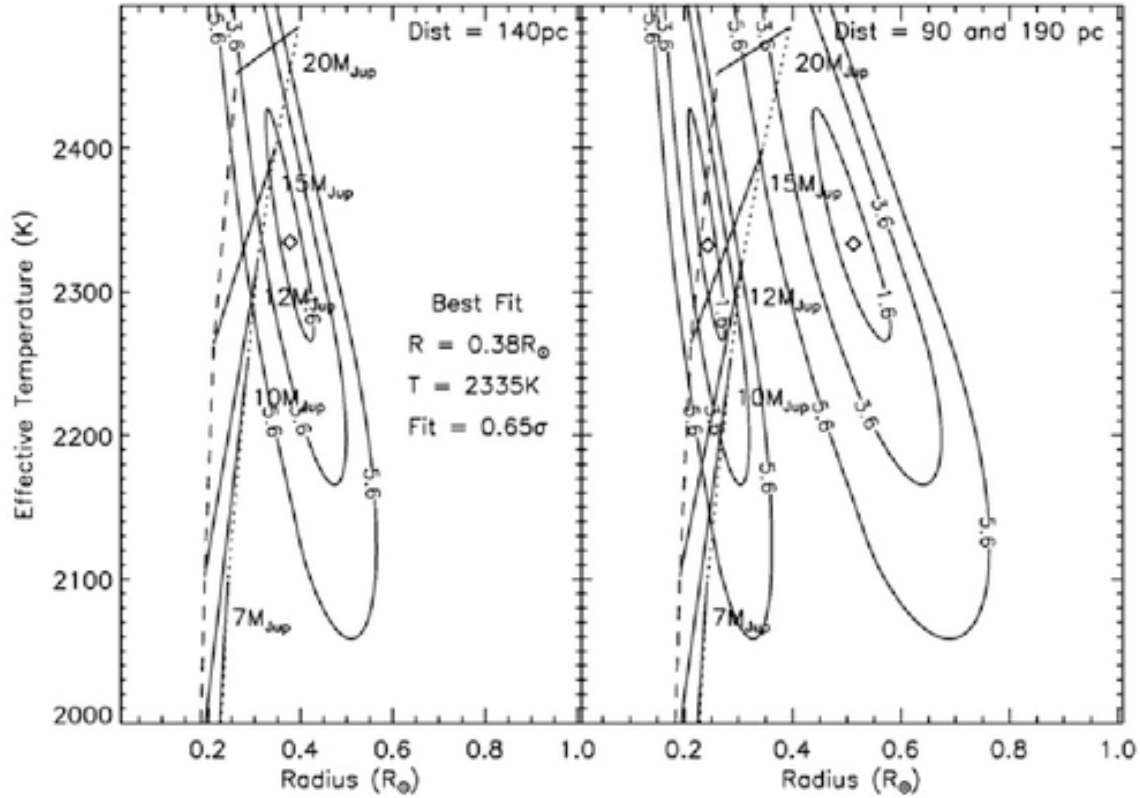


Figure 3: χ^2 contours of a temperature-radius fit for GQ Lup B. The major uncertainty remaining is the distance; two fits are shown, for the most likely distance of 140 pc (left) and 90 and 190 pc (right). The diamonds represent the best fit. Three contour levels at 1, 3, and 5 σ from the best fit are shown. Model predictions for 7MJup, 10MJup, 12MJup, 15MJup, and 20MJup and 1 Myr (dotted line) and 5 Myr (dashed line) are also shown.

3. “Extreme” adaptive optics

As shown above, current-generation AO systems are not capable of detecting any but the brightest and youngest extrasolar planets in wide orbits (if such exist.) They are limited by several main factors. The degree and speed of AO correction, set by technological limitations such as computation and deformable mirror (DM) technology, limits compensation of the atmosphere. Imperfect sensing of the wavefront due to effects such as wavefront sensor aliasing contribute both dynamic and static errors. Optical errors on individual surfaces in the AO system, especially those present only in the path taken by science light (“non-common-path” errors) can produce persistent speckle artifacts. Diffraction and optical chromaticity are also significant.

With advances in AO technology, these effects can be overcome in an AO system designed specifically for high-Strehl, high-contrast operation. Such a system will be designed to take advantage of its planned mode of operation: narrow-field observations of

bright star. Several technological innovations were required to enable such systems. Under support of this LDRD, we developed advanced AO concepts than will enable the construction of the world’s most advanced AO system, the Gemini Planet Imager (GPI, Section 4). When these technologies are brought together, they allow an AO system to remove the scattered starlight over a region close to the star, called a “dark hole”. Such technologies will also be applicable to future programmatic and non-astronomical AO projects. We discuss the key technical issues addressed by this LDRD here.

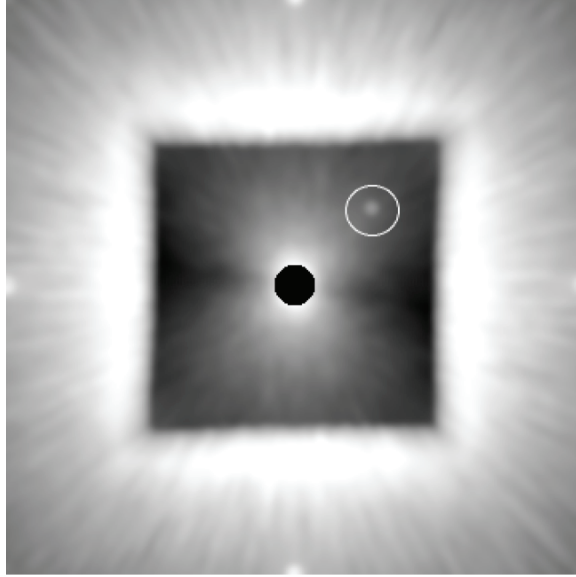


Figure 4: Simulated 20 second ExAO integration showing a 5 Jupiter-mass extrasolar planet in a 6 AU orbit around a solar-type star at 10 pc. The star is located behind an occulting spot. The square “dark hole” region, 2.6” on a side, is produced by our spatially-filtered wavefront sensor (SFWFS).

Table 1: Comparison of current Keck AO to ExAO system

Parameter	Keck	GPI
Subaperture size	0.56 m	0.18 m
Number of subapertures across pupil	16x16	44x44
Update rate	670 Hz	2000 Hz
Number of actuators on DM	349	4096
DM size	20 cm	~13 mm
Internal static wavefront error before / after calibration	200 nm / 130 nm	45-24 nm / <5 nm
WFS CCD size	64x64	160x160

3.1. Fast and efficient wavefront control

In a traditional AO system, the incoming light is sampled at sub-kHz rates by a wavefront sensor with N subapertures. That information is reconstructed into a wavefront and hence into commands for the deformable mirror. The computational requirements per

timestep for traditional wavefront reconstruction scales as N^2 ; increasing from the Keck AO system to GPI is a 30-fold increase in required computer power.

To overcome this, we developed a Fourier-transform-based wavefront control algorithm that scales as $N \log(N)$. In this approach, we reconstruct the wavefront not in terms of deformable mirror actuators but in terms of spatial frequencies – Fourier modes of the wavefront. This framework lends itself naturally to a variety of techniques to enhance the accuracy of the reconstructed wavefront. Both the atmospheric wavefront and the random noise of the wavefront sensor are “colored” signals, with different amplitudes at different spatial frequencies. Since each Fourier mode in the wavefront is independent, we can derive an unique optimal control loop for each mode that balances the relative signal and noise (Poyneer & Veran 2005). This modal gain approach is new to LLNL AO, and can reduce reconstructed wavefront noise by a factor of 2 (Figure 5.)

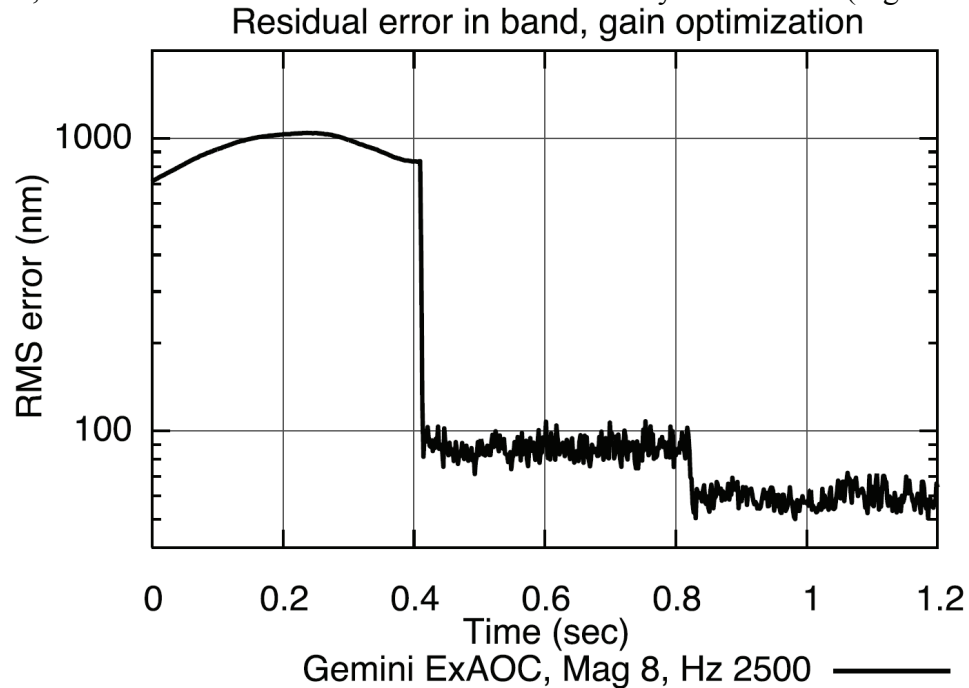


Figure 5: Time history of residual wavefront error for the optimized Fourier control. At time 0.4 seconds the AO loop closes with a simple uniform control law. The system then begins independently analyzing the signal-to-noise of each Fourier mode. At time 0.8 seconds, independent control laws are applied to individual modes to suppress noise.

3.2. *Laboratory demonstrations of advanced wavefront control*

Traditional wavefront sensors, which sample the wavefront with a discrete grid of lenslets, are subject (like any sampled signal) to aliasing – high spatial frequency components of the wavefront corrupt the low frequency measurements of interest. We devised an approach to mitigate this through spatial filtering, using the property that high spatial frequency wavefront errors scatter light to large angles (Poyneer & Macintosh 2004.) This concept is now a feature of all high-contrast AO systems on the drawing board. During the course of this LDRD we validated this concept, combined with the

Fourier reconstructor, using a testbed at the Laboratory for Adaptive Optics (LAO) at UC Santa Cruz. The LAO testbed has a 32 x 32 Boston Micromachines MEMS technology deformable mirror. As is shown in Figure 6, a high-precision interferometer is used to measure the wavefront correction provided by the MEMS, while a high-order Shack-Hartmann lenslet array is used to control the MEMS.

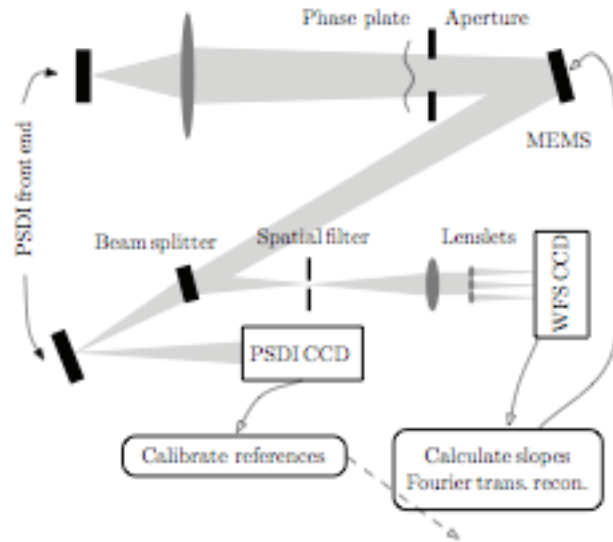


Figure 6: Schematic of the LAO testbed that is used to validate key new AO technologies.

With use of this testbed, we have verified the ability of the Fourier Transform wavefront Reconstruction (FTR), when used with the Spatially Filtered Wavefront Sensor (SFWFS), to control the MEMS to less than 1 nm RMS error. The SFWFS provides the system with accurate measurements of the phase aberration, uncorrupted by aliasing of uncontrollable high-spatial frequency errors. The SFWFS must be precisely aligned to reduce non-common-path errors. During operation, the wavefront slope measurements are reconstructed with FTR, providing an estimate of the phase compensation that the MEMS must form. We first demonstrated the ability of the FTR-SFWFS setup to correct the inherent distortion on the MEMS to less than 1 nm RMS.

Then, using etched phase plates with atmospheric-turbulence statistics, we demonstrated that the FTR-SFWFS setup can correct large phase aberrations that have substantial high-spatial frequency phase content. The correction quality is measured directly by the interferometer, which provides a direct phase measurement of the wavefront error at the MEMS plane. This signal is analyzed in the spatial frequency domain, producing a power spectral density (PSD) of the residual phase error. In our initial tests, non-linear effect due to the large phase discontinuities on the etched plates limited the correction to a few nm RMS. After calibration of the reference slopes signals (used to set the control point of the closed loop) sub-nm flattening was achieved, as is shown by the PSDs in Figure 7

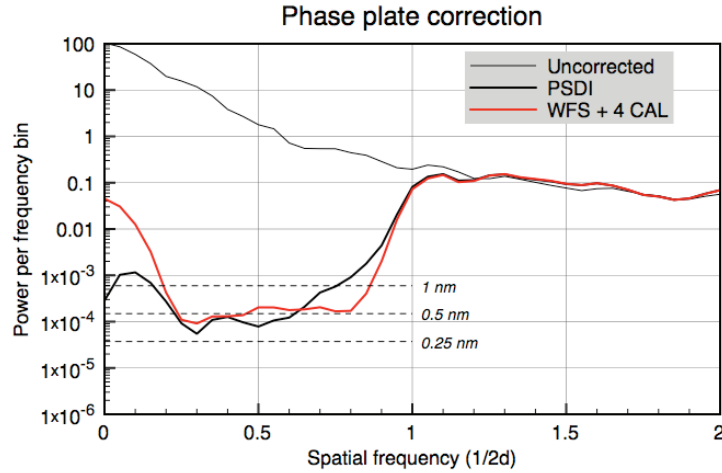


Figure 7: Radial average of spatial PSD of the residual phase after correction by an AO spatially-filtered WFS. These techniques produce a “dark hole” in the residual phase power which is $> 1000\times$ deep. For comparison, performance is also shown with a sub-nm LLNL-built interferometer (“PSDI”).

3.3. Predictive AO control

Even with the efficient Fourier control discussed above, the performance of any AO system is ultimately limited by its ability to respond to the changing wavefront errors induced by the atmosphere. In this LDRD project, we have developed a more sophisticated control algorithm that can provide even better atmospheric correction. On short timescales, the free-atmosphere-turbulence wavefront evolves under “frozen flow”, with density fluctuations embedded in distinct layers moving at the bulk wind velocity. The application of control theory techniques to AO predictive control dates back to the work of Paschall and Anderson in 1993. More recently, both Gavel and Wiberg and Le Roux et al have proposed AO controllers that predict the atmosphere. Three key weaknesses prevent these proposals from actually being implemented in a real astronomical AO system: they can generally only predict motion of a single atmospheric layer, they require a priori knowledge of the wind velocity, and they require far too much computation for a realistic AO control computer.

Our proposal for Predictive Fourier Control (PFC) solves these three problems by applying Kalman filtering to each Fourier mode of the wavefront. The Fourier modes are both spatially and temporally uncorrelated under frozen flow. This allows them to be controlled independently. The frozen flow translation of each layer of atmospheric turbulence produces a highly compact “peak” in the temporal PSD of a mode. The temporal frequency of the peak is just the dot product of the velocity vector with the frequency vector of that mode. This structure allows easy identification of multiple atmospheric layers during closed-loop operation (see Figure 8). This is in direct contrast to other basis sets, such as the Zernike modes or the actuators (shown in Figure 8). In those basis sets, the modes are correlated, and the layer structure is not easy identifiable.

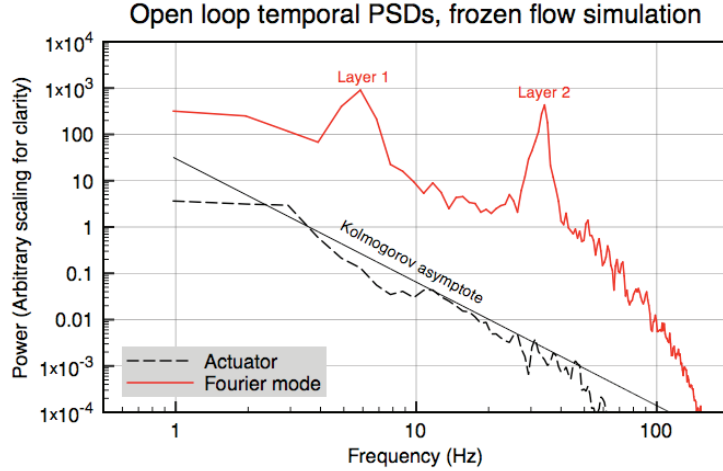


Figure 8: Frozen flow atmosphere is easily identifiable in the temporal PSD of a Fourier mode, as compared to an actuator (PSDs estimated from AO simulation data).

For each Fourier mode, the wind layers are identified from closed-loop telemetry and characterized with temporal frequencies and power levels. These parameters are used to solve the Algebraic Riccati Equation, producing the steady-state Kalman filter that predicts each mode. The predictive Kalman filter has a simple structure. First, each layer is tracked in parallel by properly predicting the delayed WFS measurements and the previous layer position on the DM. These layer estimates are then weighted and summed, and sent through a stabilizing lead filter that guarantees controller stability. Because each Fourier mode is controlled individually with a low-order filter, the computational cost of PFC is reasonable. For GPI, PFC can be implemented on existing computer hardware.

PFC allows the AO system to adapt to wind conditions and to predict the atmospheric layers. The result is significantly reduced residual error, particularly in high-order systems and when wind speeds are high. Figure 9 shows simulated coronagraphic AO images, using a condensed 3-layer wind profile for Cerro Pachon median seeing. With GPI's baseline OFC algorithm, the "butterfly" shape of the temporal lag is clearly visible in the AO-corrected "dark hole". This is because the integral controller can adjust to overall SNR, but not to specific layers. In contrast, the Kalman filtering of PFC predicts high temporal frequency wind components. This erases the wind signature and produces a symmetric, dark region for planet detection.

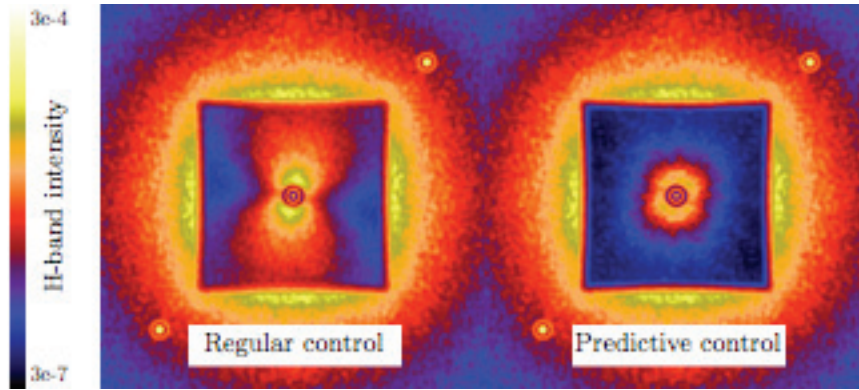


Figure 9: Simulated coronagraphic AO images comparing regular AO control to Predictive Fourier Control.

For bright-star planet-finding systems such as GPI, PFC allows fainter planets to be detected. Alternatively it can allow the same level of performance at lower frame rates with dimmer reference beacons. For most general-purpose AO systems, these reference beacons are provided by expensive custom sodium laser beacons; reducing the laser beacon power by a factor of two could translate into millions of dollars of cost reduction.

3.4. Advanced optical modeling

Traditional adaptive optics is concerned only with the analysis and correction of wavefront phase aberrations, since those dominate degraded image quality and since deformable mirrors can only easily correct phase. In the ExAO regime, however, this model is not sufficient. Due to the high quality of ExAO phase correction, a significant source of remaining scattered light (particularly within the “Dark hole” region) is the variation in the intensity of the propagating wavefront. These amplitude errors can come both from changes in the reflectivity of mirrors and from wave-optics effects, i.e. the Talbot Effect where as the aberrated wavefront propagates, mixing occurs between phase and amplitude errors. The key scale is the Talbot length. For a pure phase aberration of spatial period a at a wavelength λ , the Talbot length is $2a/\lambda$. Over a distance of one Talbot length, a pure phase error propagates into a pure amplitude error, into a phase error with the opposite sign, into an amplitude error, and then back again into the original phase error. If a phase error with random spatial frequencies is induced on an internal AO optic, particularly close to focus, by the time the light reaches the DM the phase error will have partially converted to amplitude, which is uncorrectable by the DM.

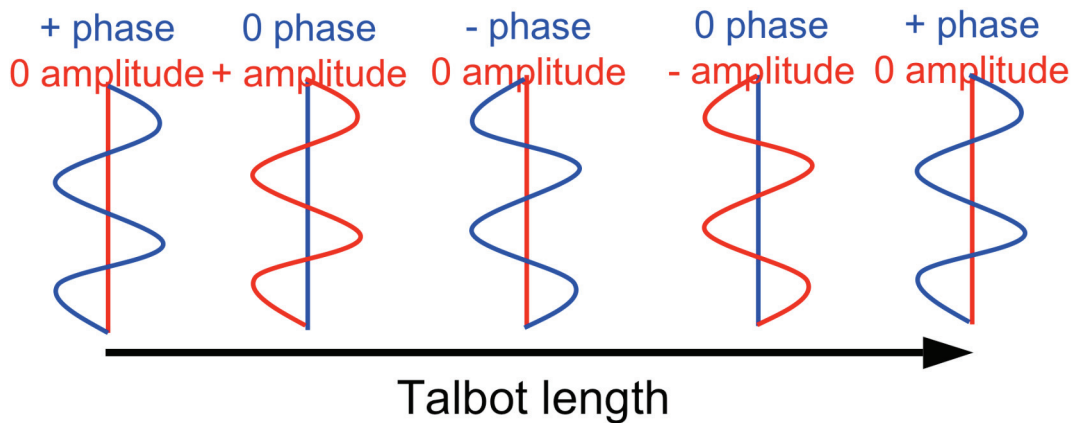


Figure 10: Illustration of the Talbot effect for a sinusoidal phase aberration

We developed end-to-end wave-optics models of the AO system to evaluate these effects. They allow us to introduce arbitrary aberrations in different planes of the system and track the optical effects through to the DM and final output. These can be used in turn to set requirements on optics quality so that amplitude mixing does not dominate final sensitivity. The same Talbot formalism discussed above also opens the possibility of correcting these errors by using multiple deformable mirrors at different locations along the beam. Such correction could be of great value to implementation of AO in high-power lasers, where phase-induced amplitude errors from different optical planes (hot spots) are a significant limitation in total power.

4. Future: the Gemini Planet Imager

The Gemini Observatory is a US/UK/Canadian facility with two 8-m telescopes (one in Chile and one in Hawaii). It is the largest US national optical/IR telescope. Gemini is operated for the National Science Foundation by the Association of Universities for Research In Astronomy (AURA.) In the Aspen process, Gemini selected an Extreme Adaptive Optics system as a candidate next-generation instrument, based in part on the compelling analysis of the LLNL-led team. Gemini/AURA funded competing conceptual design studies from a LLNL-led team and a team centered at the University of Arizona. Ultimately, LLNL's greater technical expertise led to our team's selection.

The instrument is now known as the Gemini Planet Imager (GPI). It will incorporate many of the technologies developed under this LDRD, providing the first integrated system-level implementation of advanced ExAO. It will also operate using the observational techniques we have pioneered in our existing surveys. GPI is a \$24M NSF-funded program, led by LLNL. Collaborating institutions include Canada's Herzberg Institute of Astrophysics, the NASA Jet Propulsion Laboratory, UCLA, UC Berkeley, UC Santa Cruz, the American Museum of Natural History, and University of Montreal. GPI first-light observations are expected in early 2011 at the Gemini South telescope in Chile. It is expected that LLNL will also play a major scientific role in the operation of the instrument. GPI will be capable of seeing Jupiter-mass planets on solar-system-like scales (5-50 AU) and will carry out a large-scale survey of stars in the solar

neighborhood It will also be capable of spectrally characterizing these planets to determine their temperature, gravity/mass and composition.

As discussed above, technology developed for GPI will be broadly applicable to future adaptive optics systems. In the 1990s, LLNL built an AO system for the Keck Observatory building on the LDRD-supported Laser Guide Star program, then went on to apply that technology and expertise to projects such as the DARPA CCIT effort, the Solid-State Heat Capacity Laser, biomedical AO microscopy, etc. In a similar fashion, GPI serves a cornerstone project for LLNL's AO group at the start of the 21st century and will lead to participation in future advanced AO for many applications.

5. Publications and references

Publications resulting from this LDRD are highlighted in *italics*.

Close, Laird M.; Zuckerman, B.; Song, Inseok; Barman, Travis; Marois, Christian; Rice, Emily L.; Siegler, Nick; Macintosh, Bruce; Becklin, E. E.; Campbell, Randy; Lyke, James E.; Conrad, Al; Le Mignant, David, 2007, "The Wide Brown Dwarf Binary Oph 1622-2405 and Discovery of a Wide, Low-Mass Binary in Ophiuchus (Oph 1623-2402): A New Class of Young Evaporating Wide Binaries?", 2007 Ap.J., 660, 1492

Apai, D., et al., "A survey for massive giant planets in debris disks with evacuated inner cavities", 2007 Ap.J. 672, 1196

Evans, J.W., Bruce Macintosh, Lisa Poyneer, Katie Morzinski, Scott Severson, Daren Dillon, Donald Gavel, Layra Reza 2006, "Demonstrating sub-nm closed loop MEMS flattening", Optics Express 14, 5558

Evans, J.W., Gary Sommargren, Bruce Macintosh, Scott Severson, and Daren Dillon, 2006, "Effect of wavefront error on 10-7 contrast measurements", Optics Letters, 31, 565

Fitzgerald, M., Kalas. P., Duchene, G., Pinte, C., Graham, J.R., "The AU Microscopii Debris Disk: Multiwavelength imaging and modeling", 2007 Ap.J. 670, 536

Konopacky, Q.M., Ghez, A.M., Duchene, G., McCabe, C., and Macintosh, B., "Measuring the mass of a pre-main-sequence binary star through the orbit of TWA 5A", 2007 A.J. 133, 2008

Lafreniere, D., Doyon, R., Marois, C., Nadeau, D., Oppenheimer, B., Roche, P., Rigaut, F., Graham, J., Jayawardhana, R., Johnstone, D., Kalas, P., Macintosh, B., and Racine, R., "The Gemini Deep Planet Survey", 2007 Ap.J. 670, 1367

Lowrance, P., et al., "An infrared coronagraphic survey for substellar companions", 2005 A.J. 130, 1845

Marois, C., Lafreniere, D., Macintosh, B., Doyon, R. 2006b "Accurate Astrometry and Photometry of Saturated and Coronagraphic Point Spread Functions", ApJ. 647, 612

- Marois, C., Lafrenier, D., Doyon, R., Racine, R., Nadeau, D., and Macintosh, B., “Direct exoplanet imaging and spectroscopy with an Angular Differential Imaging Technique”, 2006 *Astrophysical Journal* 641, 556
- Marois, C., Phillion, D., and Macintosh, B., “Exoplanet detection with simultaneous spectral differential imaging: effects of out-of-pupil-plane optical aberrations”, 2006c, *Advances in Adaptive Optics II, Proc SPIE* 6272
- Marois, C., Macintosh, B., Barman, T., 2007 “GQ Lup B Visible and Near-infrared photometric analysis”, *Ap.J.* 645, L151
- Marois, C., LaFreniere, D., Macintosh, B., Doyon, R., 2008 “Confidence and sensitivity limits in high-contrast imaging”, *Ap.J.* 673, 647
- Marley, M., Fortney, J., Hubickyj, O., Bodenheimer, P., Lissauer, J., “On the luminosity of young Jupiters”, 2007 *Ap.J.* 655, 541
- Neuhauser, R., et al., 2005, “Evidence for a co-moving substellar companion of GQ Lup”, *A&A* 435L, 13
- Poyneer, L. and Macintosh, B., “Spatially filtered wavefront sensor for high-order adaptive optics”, 2004 *J. Opt. Soc. Am. A* 21, 810
- Poyneer, L., and Veran, J.P., “Optimal modal fourier transform wave-front control”, 2005 *J. Opt. Soc. Am. A.*, 22, 1515
- Poyneer, L., Bauman, B., Macintosh, B., Dillon, D., and Severson, S., “Experimental demonstration of phase correction with a 32x32 MEMS mirror and spatially-filtered wavefront sensor”, 2006 *Optics Letters* 31, 293
- Poyneer, L., and Macintosh, B., 2006 “Optimal Fourier Control performance and speckle behavior in high-contrast imaging with Adaptive Optics”, *Opt. Exp.* 14, 7499
- Poyneer, L., Macintosh, B. and Veran, J.P., “Fourier transform wavefront control with adaptive prediction of the atmosphere”, 2007 *J. Opt. Soc. Am. A.*, 24, 2645
- Siegler, N., Close, L., Burgasser, A., Cruz, K., Marois, C., Macintosh, B., Barman, T., “Discovery of a 66 mas ultracool binary with laser guide star adaptive optics”, 2007 *AJ* 133, 232
- Terebey, S., et al., 2000 “The spectrum of TMR-1C is consistent with a background star”, *AJ* 119, 2341

This work was performed under the auspices of the U.S. Department of Energy by Lawrence Livermore National Laboratory in part under Contract W-7405-Eng-48 and in part under Contract DE-AC52-07NA27344.